

---

## Appendix W8.4

# Control of the Fuel-Air Ratio in an Automotive Engine

Until the 1980s, most automobile engines had a carburetor to meter the fuel so the ratio of the gasoline-mass flow to air-mass flow, or fuel-to-air ratio (F/A), remained in the vicinity of 1:15. This device metered the fuel by relying on a pressure drop produced by the air flowing through a venturi. The device performed adequately in terms of keeping the engine running satisfactorily, but it historically allowed excursions of up to 20% in the F/A. After the implementation of federal exhaust-pollution regulations, this level of inaccuracy in the F/A was unacceptable because neither excess hydrocarbons (HCs) nor excess carbon monoxide (CO) could be accepted. During the 1970s, automobile companies improved the design and manufacturing process of the carburetors so they became more accurate and delivered a F/A accuracy in the vicinity of 3% to 5%.

Through a combination of factors, this improved F/A accuracy helped lower the exhaust pollution levels. However, the carburetors were still open-loop devices because the system did not measure the F/A of the mixture entering the engine for subsequent feedback into the carburetor. During the 1980s, almost all manufacturers turned to feedback control systems to provide a much-improved level of F/A accuracy, an action made necessary by the decreasing levels of allowable exhaust pollutants. In essence, the same scheme is used currently (2025) so the catalytic converters attached to the exhaust system can remove the pollutants from the exhaust and meet the federal standards.

We now turn to the design of a typical feedback system for engine control, again using the step-by-step design outline given in Section 10.1.

**STEP 1. Understand the process and its performance.** The method chosen to meet the exhaust-pollution standards has been to use a catalytic converter that simultaneously oxidizes excess levels of exhaust carbon monoxide (CO) and unburned HCs and reduces excess levels of the oxides of nitrogen (NO and NO<sub>2</sub>, or NO<sub>x</sub>). This device is usually referred to as a three-way catalyst because of its effect on all three pollutants. This catalyst is ineffective when the F/A is much different from the stoichiometric level of 1:14.7; therefore, a feedback control system is required to maintain the F/A within  $\pm 1\%$  of that desired level. The system is depicted in Fig. W8.46.

The dynamic phenomena that affect the relationship between the sensed F/A output from the exhaust and the fuel-metering command in the intake manifold are (1) intake fuel and air mixing, (2) cycle delays due to the piston strokes in the engine, and (3) the time required for the exhaust to travel from the engine to the sensor. All these effects are strongly dependent on the speed and load of the engine. For example, engine speeds typically vary from 600 to 6000 rpm. The result of these variations is that the time delays in the system that will affect the feedback control-system behavior will also vary by at least 10:1, depending on the operating condition. The system undergoes transients as the

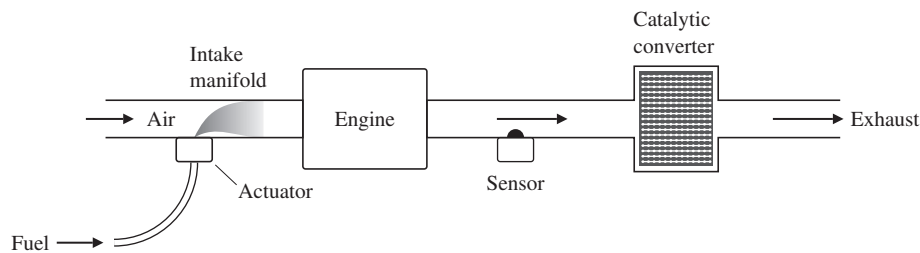
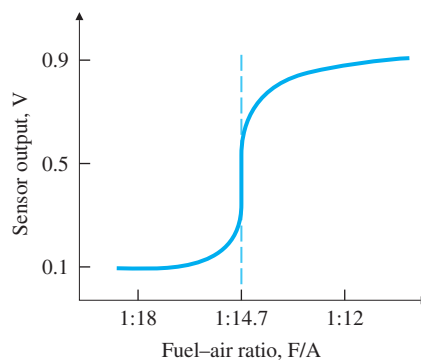


**Figure W8.46**

F/A feedback control system

Figure W8.47

Exhaust sensor output



driver demands more or less power through changes in the accelerator pedal, with the changes taking place over fractions of a second. Ideally, the feedback control system should be able to keep up with these transients.

**STEP 2. *Select sensors.*** The discovery and development of the exhaust sensor was the key technological step that made possible this concept of exhaust-emission reduction by feedback control. The active element in the device, zirconium oxide, is placed in the exhaust stream, where it yields a voltage that is a monotonic function of the oxygen content of the exhaust gas. The F/A is uniquely related to the oxygen level. The voltage of the sensor is highly nonlinear with respect to F/A (see Fig. W8.47); almost all the change in voltage occurs precisely at the F/A value at which the feedback system must operate for effective performance of the catalyst. Therefore, the gain of the sensor will be very high when the F/A is at the desired point (1:14.7), but will fall off considerably for F/A excursions away from 1:14.7.

Although other sensors have been under development for possible use in F/A feedback control, no other cost-effective sensor has so far demonstrated the capability to perform adequately. All manufacturers of production-line automobiles currently use zirconium oxide sensors in their feedback control systems.

**STEP 3. *Select actuators.*** Fuel metering is accomplished by fuel injectors in current day automobiles. The fuel injectors are either placed in the inlet port near the entrance to each cylinder or the injectors spray the fuel at high pressures directly into the combustion chamber after the inlet valve is closed. These arrangements drastically improve the accuracy of the fuel control to each cylinder compared to the throttle body injection used when feedback control was first introduced in the 1980s. Direct injection into the combustion chambers has always been used for diesel engines, but started to be used for gasoline engines about 20 years ago. It has now become quite common due to its ability to carefully shape the fuel spray and timing of the fuel injection pattern, thus allowing higher compression ratios which lead to significant improvements in fuel economy along with reductions in particulates and the

Nonlinear sensor

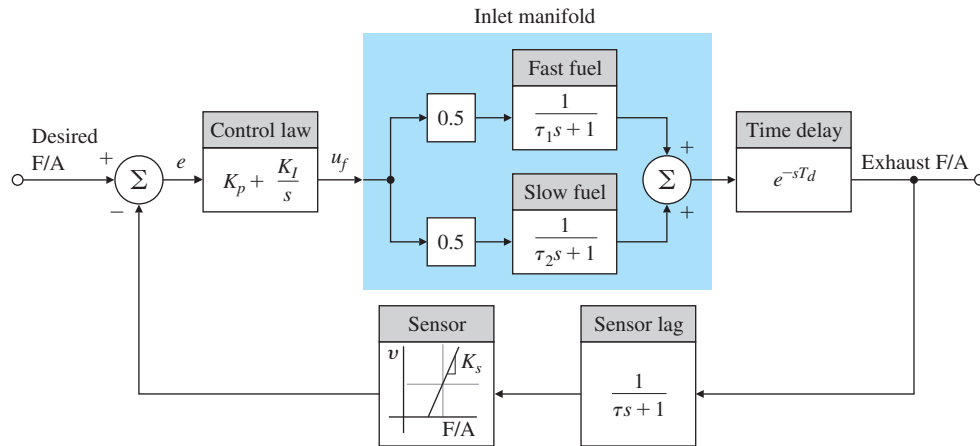


**Figure W8.48**

Block diagram of an F/A control system

other exhaust emissions. Direct injection also minimizes the time delay thus providing better engine response and more accurate fuel control, which also helps economy and emissions.

**STEP 4. Make a linear model.** The sensor nonlinearity shown in Fig. W8.47 is severe enough that any design effort based on a linearized model of it should be used with caution. Figure W8.48 shows a block diagram of the system, with the sensor shown to have a gain  $K_s$ . The time constants  $\tau_1$  and  $\tau_2$  indicated for the inlet-manifold dynamics represent, respectively, fast-fuel flow in the form of vapor or droplets and slow-fuel flow in the form of a liquid film on the manifold walls. The time delay is the sum of (1) the time it takes the pistons to move through the four strokes from the intake process until the exhaust process and (2) the time required for the exhaust to travel from the engine to the sensor located roughly 1 ft away. A sensor lag with time constant  $\tau$  is also included in the process to account for the mixing that occurs in the exhaust manifold. Although the time constants and the delay time change considerably, primarily as a function of engine load and speed, we will examine the design at a specific point where the values are

$$\begin{aligned}\tau_1 &= 0.02 \text{ sec}, & T_d &= 0.2 \text{ sec}, \\ \tau_2 &= 1 \text{ sec}, & \tau &= 0.1 \text{ sec}.\end{aligned}$$

In an actual engine, designs would be carried out for all speed loads.

**STEP 5. Try a lead-lag or PID controller.** Given the tight error specifications and the wide variations in the required fuel command  $u_f$  due to varying engine-operating conditions, an integral-control term is mandatory. With integral control, any required steady-state  $u_f$  can be provided when the error signal  $e = 0$ . The addition of a proportional term, although not often used, allows for an increase (doubling) in the

bandwidth without degrading steady-state characteristics. In this example, we use a control law that is proportional plus integral (PI). The output from the control law is a voltage that drives the injector's pulse former to give a fuel pulse whose duration is proportional to the voltage. The controller transfer function can be written as

$$D_c(s) = K_p + \frac{K_I}{s} = \frac{K_p}{s}(s + z), \quad (\text{W8.35})$$

where

$$z = \frac{K_I}{K_p},$$

and  $z$  can be chosen as desired.

First, let us assume the sensor is linear and can be represented by a gain  $K_s$ . Then, we can choose  $z$  for good stability and good response of the system. Figure W8.49 shows the frequency response of the system for  $K_s K_p = 1.0$  and  $z = 0.3$ , while Fig. W8.50 shows a root locus

**Figure W8.49** Bode plot of a PI F/A controller

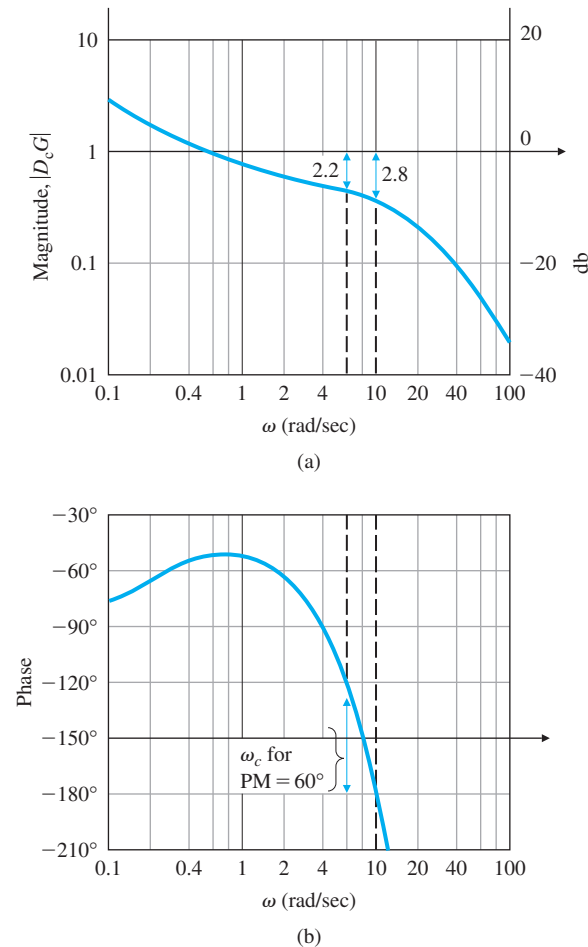
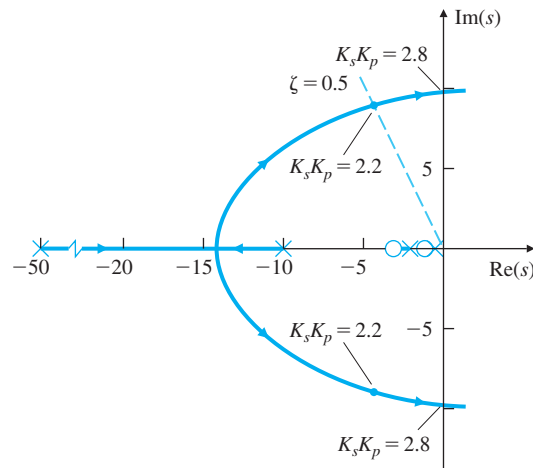


**Figure W8.50**  
Root locus of a PI F/A  
controller



of the system with respect to  $K_s K_p$  with  $z = 0.3$ . Both analyses show the system becomes unstable for  $K_s K_p \cong 2.8$ . Figure W8.49 shows to achieve a phase margin of approximately  $60^\circ$ , the gain  $K_s K_p$  should be  $\sim 2.2$ . Figure W8.49 also shows this produces a crossover frequency of 6.0 rad/sec ( $\sim 1$  Hz). The root locus in Fig. W8.50 verifies this candidate design will achieve acceptable damping ( $\zeta \cong 0.5$ ).

#### Complications of nonlinearity

Although this linear analysis shows that acceptable stability at a reasonable bandwidth ( $\sim 1$  Hz) can be achieved with a PI controller, a look at the nonlinear sensor characteristics (see Fig. W8.47) shows that this indeed may not be achievable. Note the slope of the sensor output is extremely high near the desired setpoint, thus producing a very high value of  $K_s$ . Therefore, lower values of the controller gain  $K_p$  need to be used to maintain the overall  $K_s K_p$  value of 2.2 when including the effect of the high sensor gain. On the other hand, a value of  $K_p$  low enough to yield a stable system at F/A = 1 : 14.7 (= 0.068) will yield a very sluggish response to transient errors that deviate much from the setpoint, because the effective sensor gain will be reduced substantially. It is therefore necessary to account for the sensor nonlinearity in order to obtain satisfactory response characteristics of the system for anything other than minute disturbances about the setpoint. A first approximation to the sensor is shown in Fig. W8.51. Because the actual sensor gain at the setpoint is still quite different from its approximation, this approximation will yield erroneous conclusions regarding stability about the setpoint; however, it will be useful in a simulation to determine the response to initial conditions.

**STEP 6. Evaluate/modify plant.** The nonlinear sensor is undesirable; however, no suitable linear sensor has been found.

**STEP 7. Try an optimal controller.** The response of this system is dominated by the sensor nonlinearity, and any fine tuning of the control needs to account for that feature. Furthermore, the system dynamics

**Figure W8.51** Sensor approximation

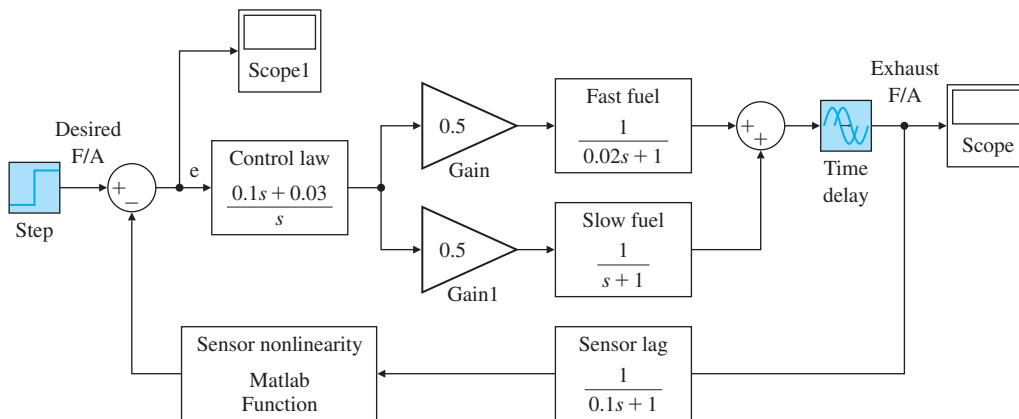
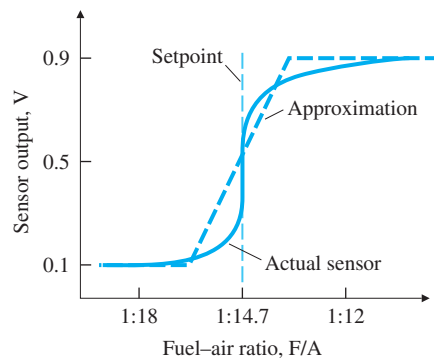


**Figure W8.52**

Closed-loop nonlinear simulation implemented in Simulink

Source: Reprinted with permission of The MathWorks, Inc.

are relatively simple, and it is unlikely that an optimal design approach will yield any improvement over the PI controller used. We will thus omit this step.

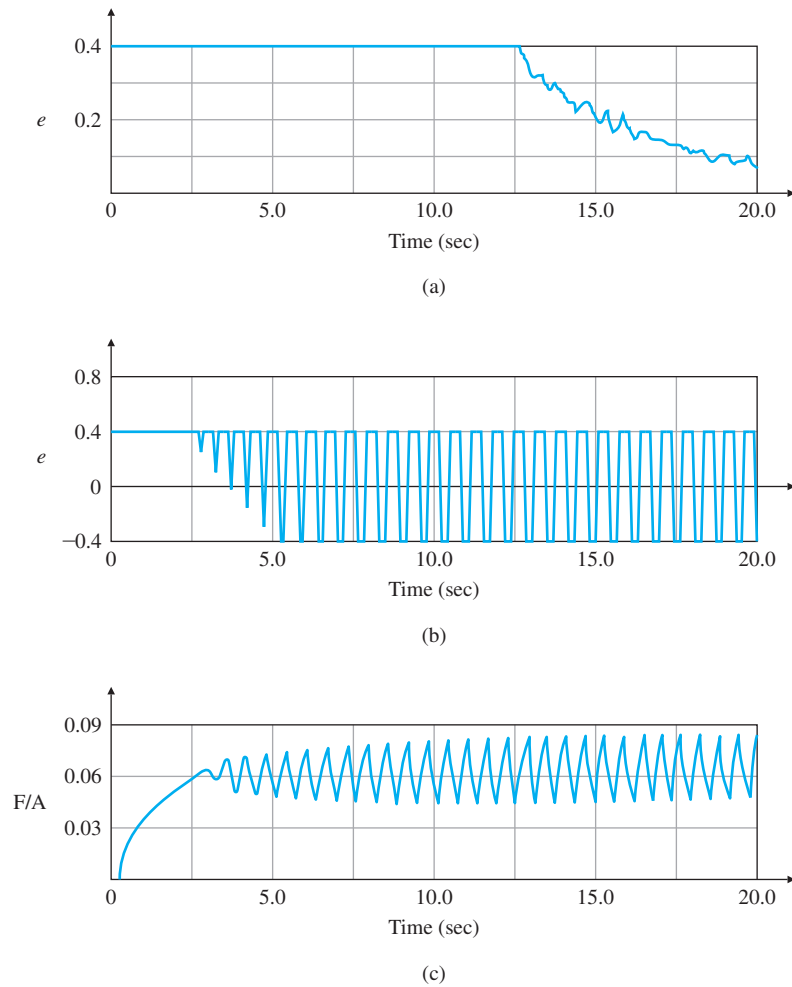
#### Simulink nonlinear simulation

**STEP 8. Simulate design with nonlinearities.** The nonlinear closed-loop simulation of the system implemented in Simulink is shown in Fig. W8.52. The Matlab function *fas* implements the approximate non-linear sensor characteristics of Fig. W8.51,

```
function y = fas(u)
if u < 0.0606,
    y = 0.1;
elseif u < 0.0741,
    y = 0.1 + (u - 0.0606) * 20;
else y = 0.9;
end
```

Figure W8.53(a) is a plot of the system error using the approximate sensor of Fig. W8.51 and  $K_p K_s = 2.0$ . The slow response is apparent with

**Figure W8.53** System response with nonlinear sensor approximation



12.5 sec before the error comes out of saturation and a time constant of almost 5 sec once the linear region is reached. In real automobiles, these systems are operated with much higher gains. To show these effects, a simulation with  $K_p K_s = 6.0$  is plotted in Fig. W8.53(b, c). At this gain the linear system is unstable, and up until about 5 sec, the signals grow. The growth halts after 5 sec due to the fact that, as the input to the sensor nonlinearity gets large, the *effective* gain of the sensor decreases due to the saturation, and eventually, a limit cycle is reached. The frequency of this limit cycle corresponds to the point at which the root locus crosses the imaginary axis and has an amplitude such that the total effective gain of  $K_p K_{s,eq} = 2.8$ . As described in Section 10.3, the effective gain of a saturation for moderately large inputs can be computed and is given by the describing function to be approximately  $4N/\pi a$ , where  $N$  is the saturation level and  $a$  is the amplitude of the input signal. Here  $N = 0.4$ , and if  $K_p = 0.1$ , then  $K_{s,eq} = 28$ . Thus, we predict an input signal amplitude of  $a = 4(0.4)/28\pi = 0.018$ . This value is closely verified by



the plot of Fig. W8.53(c), the input to the nonlinearity in this case. The frequency of oscillation is also nearly 10.1 rad/sec, as predicted by the root locus in Fig. W8.50.

In the actual implementation of F/A feedback controllers in automobile engines, sensor degradation over thousands of miles of use is of primary concern, because the federal government mandates that the engines meet the exhaust-pollution standards for the first 50,000 mi. In order to reduce the sensitivity of the average setpoint to changes in the sensor output characteristics, manufacturers typically modify the design discussed here. One approach is to feed the sensor output into a relay function [see Fig. 10.6(b)], thus completely eliminating any dependency on the sensor gain at the setpoint. The frequency of the limit cycle is then solely determined by controller constants and engine characteristics. Average steady-state F/A accuracy is also improved. The oscillations in the F/A are acceptable because they are not noticeable to the car's occupants. In fact, the F/A excursions are beneficial to the catalyst operation in reducing pollutants.

The addition of catalytic converters, along with much improved fuel control, has resulted in a dramatic decrease in exhaust pollutants along with much improved fuel efficiency in cars and trucks using IC engines.